Contents list available at CBIORE journal website

International Journal of Renewable Energy Development

Journal homepage: https://ijred.cbiore.id

Research Article

Enhancing solid fuel potential of water hyacinth: A study on chemical modification through composting and demineralization

Mustaghfirin Mustaghfirin[a], Dede Hermawan[a*], Deded Sarip Nawawi[a], Sukma Surya Kusumah[b*], Maya Ismayati[b], Jajang Sutiawan[b], Riska Surya Ningrum[b], Bramantyo Wikantyoso[c,d]

[a]*Study Program of Forest Product Science and Technology, Department of Forest Products, Faculty of Forestry and Environment, IPB University, Bogor, Indonesia*

[b]*Research Center for Biomass and Bioproduct, National Research and Innovation Agency, Tanggerang Selatan, Indonesia*

[c]*Research Center for Applied Zoology, National Research and Innovation Agency, Cibinong, Indonesia*

[d]*Cryo-Electron Microscopy Facility, National Research and Innovation Agency, Cibinong, Indonesia*

Abstract. Rapid growth makes water hyacinth (WH) an exceptional biomass resource, but its low calorific value and elevated ash content hinder its application as a sustainable green energy source. This study aims to enhance the quality of water hyacinth as a solid fuel by increasing lignin content through composting and decreasing ash content by demineralization. The composting period for water hyacinth was modified to 4, 7, 11, and 15 days, followed by a demineralization process employing two solvents: water and 5% nitric acid (HNO_3). Proximate, ultimate, and chemical studies were conducted on water hyacinth before and following treatment to ascertain its specific alterations. This study indicates that after 15 days of composting, the lignin fraction increased from 10.01% to 15.14%. Demineralization employing a combination of water and nitric acid can substantially reduce ash content (19.4%). The demineralization of raw materials during composting is more efficacious in diminishing ash content than the demineralization of raw materials before composting. The most significant reduction was 46.17%, observed in the 11-day WH composting, where the ash content decreased from 22% to 11.84%. According to the results, modified WH is a viable raw material for solid fuel due to its enhanced lignin content and reduced ash level.

Keywords: biomass energy, wood pellets, composting, demineralization

Received: 12th June 2025; Revised: 29th Oct 2025; Accepted: 5th Dec 2025; Available online: 28th Dec 2025

1. Introduction

Global energy use increases steadily each year. Forecasts indicate that Indonesia will need 1.780 million barrels of oil equivalent (BOE) by 2030 and 4.569 million BOE by 2050, mostly to meet increasing industrial and transportation requirements (Kementerian and ESDM 2024). In 2023, fossil fuels, including coal (40.46%), petroleum oil (30.18%), petroleum gas (16.28%), and renewable energy (RE) (13.09%), continue to dominate Indonesia's energy needs. We anticipate an increase in the share of renewable energy in the energy mix, with a production goal of approximately 23% by 2025 (Kementerian and ESDM 2024). Indonesia is promoting biomass energy as a potential renewable energy source (Perpres No. 5, 2006). Biomass energy is considered carbon neutral, as the CO_2 emitted during combustion is offset by the CO_2 absorbed during plant growth (Ahamer 2022). Moreover, biomass typically contains lower levels of sulfur and nitrogen compared to fossil fuels, resulting in reduced emissions of SO_x and NO_x during combustion (Krzywanski *et al.* 2022). The variability of biomass influences the quality of biomass energy owing to disparities in its chemical composition and calorific value (Esteves *et al.* 2023), necessitating further investigation into biomass's chemical and calorific properties.

Water hyacinth (*Eichhornia crassipes*) is a commonly available biomass source. Its fibrous composition consists of approximately 7.24% lignin, 19.51% hemicellulose, and 33.17% cellulose (Hemida *et al.* 2024). Moreover, the fiber consists of chemical elements: carbon (C) (34.12%), hydrogen (H) (5.07%), and oxygen (O) (39.95%) (R Darmawan *et al.* 2021). (Huang *et al.* 2018) indicated that WH possessed a calorific value (CV) of roughly 3527.75 cal/g, an ash content (AC) of 16.35%, a fixed carbon (FC) of 17.4%, and a volatile matter (VM) of 56.3%. Multiple studies have already examined the utilization of WH for biomass energy. (Wichianphong N and Maison W 2020) developed bio-pellets from water hyacinth (WH) by amalgamating it with coffee grounds. The bio-pellets made only of pure WH have a calorific value of 3296.07 cal/g. Combining water hyacinth and coffee grounds in a 60:40 ratio yields bio-pellets with a heightened calorific value of 4105.76 cal/g. (Hudakorn and Sritrakul 2020) produce bio-pellets from pure WH, demonstrating a calorific value of 3508.65 cal/g. The current value is below the SNI requirement, which mandates that bio-pellets have a calorific value exceeding 4000 cal/g.

* Corresponding author
Email: dedehe@apps.ipb.ac.id (D. Hermawan); sukmo02@brin.go.id (S.S. Kusumah)

https://doi.org/10.61435/ijred.2026.61468
ISSN: 2252-4940/© 2026.The Author(s). Published by CBIORE

Velázquez-Araque *et al.* (2020) used WH with banana peel in their bio-pellet, achieving a calorific value of 3790.48 cal/g. Zikri *et al.* (2018) enhanced the calorific value of the bio-pellets to 4776.92 cal/g by incorporating 10%–15% damar rubber into the WH.

Various parameters, including chemical composition, moisture content, ash content, volatile matter, fixed carbon, density, and processing techniques, affect the calorific value of biomass (Mustamu and Pari 2018; Parikh *et al.* 2005; Wistara *et al.* 2020). The chemical components of biomass, including cellulose, hemicellulose, and lignin, serve as indicators for evaluating its energy potential. Among these components, carbon (C) has the most substantial influence on calorific value (Nawawi *et al.* 2018). Composting can modify the chemical composition of biomass and increase the lignin concentration of raw materials (Barneto *et al.* 2009). The principal objective of converting organic materials into mulch is to improve soil nutrition levels. Microorganisms utilize the organic matter for nourishment and energy, excreting extracellular hydrolytic enzymes to facilitate the degradation of organic materials (Ratih *et al.* 2018). During the earliest phase of composting, microorganisms produce essential carbon compounds, such as monosaccharides, salts, and lipids. In the next phase, they will break down more complex molecules, including hemicellulose, cellulose, and lignin. By meticulously adjusting the composting duration, we will confine the composting process to simple sugars, hemicellulose, and cellulose, excluding lignin, which has the highest carbon concentration (Wu *et al.* 2022).

The objective of this study is to enhance the quality of water hyacinth as a solid fuel by increasing lignin content and reducing ash content through demineralization (Jiang *et al.* 2013; Kukuruzović *et al.* 2023; Singhal *et al.* 2021). According to Singhal *et al.* (2021), immersing biomass in water at 50 °C for 10 minutes resulted in an ash reduction of up to 45%. Similarly, Jiang *et al.* (2013) reported that soaking rice straw in 5% nitric acid (HNO_3) for 2 hours at room temperature led to a significant ash reduction of approximately 55%. Furthermore, Kukuruzović *et al.* (2023) demonstrated that immersing soybean and rice straw in 1% HNO_3 for 30 minutes decreased ash content by 40–90%, depending on the biomass type. Washing with water alone removes just water-soluble minerals. In contrast, acid washing can dissolve both soluble and insoluble minerals, improving efficiency but potentially jeopardizing the physicochemical properties of the raw materials (Jiang *et al.* 2013).

2. Materials and Methods

2.1 Material preparation

Water hyacinth (WH) (*Eichhornia crassipes*) was collected from the District of Pekalongan, Central Java Province, Indonesia. The WH was chopped to obtain a particle size of approximately 2-3 cm. The WH particles were composted using a composting starter consisting of a microorganism solution (EM4), which included 20 ml of EM4, 20 ml of molasses, and 1000 ml of water (PT. Songgo Langit Persada). The composted WH was subjected to drying and milling until it passed through a 60-mesh sieve. The final step of preparation involved demineralization. A 5% nitric acid (HNO3) solution was employed for the demineralization of the WH.

2.2 Treatment of water hyacinth

The treatment for WH consists of two phases. The WH was initially composted using the EM4 activator (Ratih *et al.* 2018). The WH particles were air-dried for two days and subsequently combined with 10% w/w rice bran and 2 ml/kg of EM4 activator solution. The composting duration was varied across four intervals: 4, 7, 11, and 15 days, based on an effective decomposition process (1 week) and significant alterations in the C/N ratio (15 days) (Agung Astuti 2016). The ambient temperature, as well as the internal temperature and humidity of the compost pile, were monitored daily using a thermohygrometer. The compost pile was turned on the seventh day to ensure adequate aeration, which facilitated uniform oxygen distribution and heat dissipation during the composting process. This procedure also helped maintain optimal microbial activity and prevented the accumulation of organic acids that could otherwise cause an excessive drop in pH. The WH was dried to achieve a moisture content below 10%, followed by milling with a disc mill and sieving to obtain a particle size of 60 mesh.

The second stage entails demineralization, employing a 5% HNO3 solution and aquades for a period of 10 minutes. The water hyacinth, composted and weighing up to 50 g, is subjected to cleaning with a 5% HNO3 solution and aquades at ambient temperature. The solution-to-weight ratio is 10 ml per gram, and the mixture is agitated for 10 minutes. After the demineralization process using a 5% HNO_3 solution, the materials were thoroughly rinsed with distilled water until the filtrate reached a neutral pH. The solid residues were then oven-dried at 60 °C for two days. Only the solid fraction was collected and subjected to further analysis, while the water- or acid-soluble fractions were excluded from subsequent evaluations. Table 1 presents the composting treatment of water hyacinth.

2.3 Characterization of Water Hyacinth

The treated WH was evaluated by analysis of proximate, ultimate, chemical components, and calorific value. The analysis involved quantifying moisture content, ash content, volatile matter, and fixed carbon. The moisture, volatile matter, and ash content were determined according to a previous study (Putri *et al.* 2024). The carbon, hydrogen, nitrogen, and sulfur components were measured by using a Thermofisher Scientific Smart Organic Elemental Analyzer. The chemical components of WH, including lignin, cellulose, and hemicellulose contents, were determined according to a previos study (Murda *et al.* 2022). The calorific values were determined using a bomb calorimeter. Three repetitions of each exam are conducted.

2.4 Scanning Electron Microscopy Observation

The ultrastructural observations were conducted on untreated WH samples, composted samples, and those treated with distilled water or nitric acid. Samples were mounted on copper stubs using carbon tape. During mounting, the stubs were tilted

Table 1
Composting treatment of water hyacinth

Material	0 day	4 days	7 days	11 days	15 days
Composted	E0	E4	E7	E11	E15
Demineralized (water)	DWE0	DWE4	DWE7	DWE11	DWE15
Demineralized (HNO_3 5%)	DAE0	DAE4	DAE7	DAE11	DAE15

at approximately 45° to ensure even sample distribution. Before observation, the samples were gold-coated using an ion coater (Eiko IB-2, Japan), operated at 6 mA under vacuum for 4 minutes. The coated samples were then examined using a scanning electron microscope (SEM; JEOL JSM-IT200, Japan) at magnifications of 2000×, 4000×, and 10,000×. The electron beam was operated at 5 kV under high vacuum conditions.

2.5 Fourier transform infrared spectrometry (FTIR) analysis

An examination of the WH sample was undertaken to find modifications in its chemical structure concerning functional groups. The analysis is performed using an FTIR (PerkinElmer 4000) apparatus. Samples were analyzed using the Universal Attenuated Total Reflectance (UATR) accessory by inserting 2 mg specimens. The spectrum was captured at a wavelength at a temperature of 24 °C.

2.6 X-ray diffraction (XRD) Analysis

X-ray diffraction is employed to ascertain the crystallinity of the WH sample. The X-ray diffraction data are acquired using the PerkinElmer XD-2 (PerkinElmer 4000) instrument. The scanning rates are established at 2° per minute, and data is collected within the 10° to 60° range. The crystallinity degree (Crl, %) was calculated using the following formula (Liao *et al.* 2016):

$$\text{Crl (\%)} = \frac{\text{Icr}}{\text{Icr + Iam}} \times 100$$

Where:

Icr = Intensity of crystalline area
Iam = Intensity of amorphous area

2.7 Pyrolysis gas chromatography/mass spectrometry (PyGCMS) analysis

PyGC-MS was conducted to identify and distinguish the fast pyrolysis by-products. About 5 mg of WH samples were analyzed by pyrolysis-gas chromatography-mass-spectrometry (PyGC-MS) with n-eicosane (0.1 µg) as an internal standard. When the temperature of the cracking reactor remained constant at 600 °C, the sample was sent to the reactor. The carrier gas was helium, while the cracking duration was 24 s at 600 °C. The temperature of the transfer line between the cracking reactor and the gas chromatography was set to 300 °C. The chromatographic column used to separate the volatiles was SH-Rxi-5Sil MC Cap, column 30m,0.25mm, 0.25um. The procedure of adjusting the GC temperature was as follows: the column was kept constant for 2 min at 50 °C, heated up to 300 °C at a heating rate of 5 °C/min, and kept constant for 20 min. The carrier gas flow rate was 1.5 mL/min, and the split ratio was 1:15. The MS was performed in electron ionization (EI) mode under the full scan mode.

2.8 Statistical Analysis

All experimental data were checked for consistency prior to statistical analysis. A one-way analysis of variance (ANOVA) was performed to evaluate the significance of variations among variables and treatments. Statistical significance was determined at a 95% confidence level, where differences were considered significant if $p < 0.05$, indicating that the observed variations were unlikely to result from random error. When significant effects were detected, Duncan's Multiple Range Test (DMRT) was applied as a post-hoc test to identify which treatment means differed significantly. Treatments followed by different letters were considered statistically distinct. Each treatment was conducted in triplicate, and the results were expressed as mean ± standard deviation prior to statistical analysis to ensure accurate representation of data variability. All statistical analyses were performed using IBM SPSS Statistics version 22.

3. Results and Discussion

3.1 Parameters of the water hyacinth composting process

The EM4 activator was used for a period of 15 days to facilitate the composting process. The compost temperature increased from 31.60°C to 54°C on the second day, reaching its highest point of 63.70°C on the third day. It then progressively decreased to 32°C by the 15th day, as shown in Figure 1. The rise in the initial compounding temperature signifies the presence of intense microbial activity during the decomposition of organic matter at the start of composting. This is when microbe respiration takes place in the early stage of the composting process (Ratih *et al.* 2018). During the initial phase of composting, bacteria will utilize basic carbon molecules such as monosaccharides, amino acids, and lipids. The abundance of these molecules will diminish, leading to an increased microbial

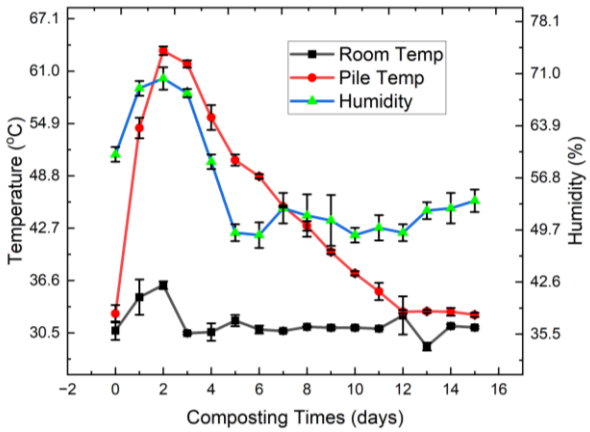

Fig. 1. Water hyacinth composting conditions during the 15 day process.

Table 2
Chemical components of water hyacinth after composting (0, 4, 7, 11, and 15)

Components	Composting time (days)				
	0	4	7	11	15
Cellulose (%)	31.0800^{d}	28.4000^{c}	26.6500^{b}	25.9300^{b}	22.6200^{a}
Hemicellulose (%)	28.5500^{d}	22.1600^{c}	19.4500^{b}	16.7600^{a}	16.2400^{a}
Lignin (%)	10.59^{a}	12.77^{b}	13.74^{c}	14.75^{d}	14.97^{d}
Lignin Demineralization with water (%)	11.4462^{a}	13.2058^{b}	13.5117^{bc}	14.5344^{cd}	15.1949^{d}
Lignin Demineralization with HNO_3 5% (%)	13.2031^{a}	14.1705^{b}	14.1770^{b}	14.9521^{b}	16.4054^{c}
Selulosa (%)	31.0800^{d}	28.4000^{c}	26.6500^{b}	25.9300^{b}	22.6200^{a}

* Treatment values followed by different letters indicate a significant difference at the 5% level.

degradation of more intricate compounds, such as hemicellulose, cellulose, and lignin. The process of breakdown is slowed down by complicated material decomposition due to the involvement of multiple enzymes acting together completely and synergistically.

Water hyacinth has a suboptimal carbon-to-nitrogen ratio of 71.64 for composting, while the ideal ratio for composting is often about 30 (Yang *et al.* 2021). The composting process is hindered by the high C/N ratio, resulting in slow progress due to insufficient nitrogen and raw materials. The growth of decay bacteria is hindered when there are insufficient levels of nitrogen, as nitrogen is essential for the synthesis of proteins, amino acids, and nucleic acids that the bacteria require (Azis *et al.* 2023). The C/N ratio drops from 71.64 to 26.37 during the composting process, as observed on day 15, and the cellulose/lignin ratio on day 15 is 1.59 (Figure 1). These findings suggest that the composting process is progressing satisfactorily, although it is not yet fully mature.

3.2 Chemical components of water hyacinth

The water hyacinth is an aquatic plant that floats on the water's surface and has permeable stems akin to cork. Table 2 presents the lignin content of WH, which is comparatively low (10.57%) compared to common biomass for energy, such as Calliandra 28.8% (Saputra *et al.* 2022). The other chemical components of WH were a content of cellulose 31.08%, hemicellulose 28.55%, extractives 14.06%, and miscellaneous components 16.6%. Lignin considerably affects calorific value owing to its elevated carbon content relative to cellulose and hemicellulose (Nawawi *et al.* 2018). Lignin possesses a calorific value between 5556 and 6110 cal/g, markedly exceeding the calorific value of holo-cellulose at 4443 cal/g (Nawawi *et al.* 2018). Biomass with high lignin content inherently has a high calorific value (Nawawi *et al.* 2018). Therefore, increasing the lignin content in biomass may yield biomass with an elevated calorific value.

The hemicellulose content decreased by 22.38% on day 4, while cellulose decreased by 8.62%. This reduction coincided with the temperature rise to the thermophilic phase, indicating intense activity of hydrolytic microorganisms. Hemicellulose, being an amorphous polysaccharide with easily cleavable glycosidic linkages (such as xylan, arabinan, and mannan), is more susceptible to enzymatic hydrolysis by xylanase and hemicellulase than cellulose, which possesses a more crystalline structure. From day 7 to day 15, the degradation rate of cellulose and hemicellulose slowed, as most of the readily available substrates had been decomposed. By day 15, cellulose and hemicellulose contents decreased to 22.62% and 16.24%, respectively, indicating that approximately 27–43% of the carbohydrate fraction had been decomposed. This mechanism was accompanied by a relative increase in lignin content due to the loss of polysaccharide fractions (Liang *et al.* 2021).

The lignin content increased by 41.63% after 15 days of composting. This result is consistent with the findings of Barneto *et al.* (2009), who reported a 24% increase in lignin content during the composting of Leucaena. This increase does not indicate the formation of new lignin, but rather a relative accumulation resulting from the faster degradation of cellulose and hemicellulose components. During the composting process, significant chemical transformations occur within the lignocellulosic matrix, particularly in the hemicellulose and cellulose fractions, which are more easily degraded than lignin. The amorphous structure of hemicellulose facilitates enzymatic hydrolysis into simple sugars such as xylose, arabinose, and glucose through the activity of xylanase and hemicellulase. Meanwhile, more crystalline cellulose undergoes gradual depolymerization into oligosaccharides and glucose via cellulase activity (Wu *et al.* 2022). These simple sugars are subsequently oxidized by microorganisms into organic acids (e.g., acetic and lactic acids), carbon dioxide, and water, leading to a substantial reduction in the proportion of non-lignin carbon fractions.

Demineralization showed a significant effect on lignin content. The lignin content increased by 31% in samples washed with water and by 26% in those treated with 5% nitric acid (HNO_3). This increasing trend is primarily attributed to the removal of alkali and alkaline earth metals such as K, Na, Ca, and Mg (Sommersacher *et al.* 2015). However, the increase in lignin after acid washing was lower than that observed with water washing. This is because nitric acid not only reacts with mineral components but also interacts with the lignocellulosic matrix. Nitric acid is capable of cleaving ether linkages (β–O–4 and α–O–4) and carbon–carbon bonds between phenylpropane units in the lignin structure, producing water-soluble aromatic compounds such as vanillic acid, syringic acid, and p-hydroxybenzoic acid (Usino *et al.* 2023). These oxidative reactions result in partial lignin degradation and solubilization into the filtrate, thereby decreasing the measured lignin content in the remaining solid fraction.

3.3 Ultimate of Water Hyacinth

The ultimate analysis of water hyacinth revealed significant changes in the elemental composition—carbon (C), nitrogen (N), hydrogen (H), sulfur (S), and oxygen (O)—throughout the 0–15 day composting period (Table 3). The carbon content decreased by 7.5%, indicating the oxidation of organic carbon into CO_2 during microbial respiration. In contrast, nitrogen increased sharply by up to 150%, suggesting nitrogen fixation and microbial biomass accumulation. Hydrogen content decreased by 6.9%, consistent with the degradation of carbohydrates and the loss of volatile compounds. In comparison, sulfur increased by 19%, likely due to the concentration effect following the decomposition of organic matter and mineralization of sulfur-containing compounds.

The decrease in carbon content indicates the degradation of organic compounds, particularly the hemicellulose and cellulose fractions, which are more readily decomposed by

Table 3
Ultimate of water hyacinth after composting (0, 4, 7, 11, and 15)

Components	Composting time (days)				
	0	4	7	11	15
Nitrogen (%)	0.5086[a]	1.2930[b]	0.9722[b]	1.1309[b]	1.2798[b]
Carbon (%)	36.4315[c]	35.3789[b]	33.7974[a]	33.6977[a]	33.7507[a]
Hydrogen (%)	4.9937[b]	4.9188[b]	4.7326[a]	4.6483[a]	4.6752[a]
Sulfur (%)	1.3388[a]	1.3290[a]	1.3524[a]	1.5071[b]	1.5931[b]
Oxygen (%)	40.1264[c]	38.9625[b]	40.3596[c]	37.0168[a]	37.3648[a]
H/C ratio	1.6452[a]	1.6688[a]	1.6803[a]	1.6552[a]	1.6625[a]
O/C ratio	0.8263[a]	0.8264[a]	0.8957[b]	0.8239[a]	0.8304[a]

* Treatment values followed by different letters indicate a significant difference at the 5% level.

microbial activity than lignin. During this process, carbon is released into the atmosphere as CO_2 through microbial respiration (Bernal *et al.* 2009). Similarly, Tuomela *et al.* (2000) reported that microorganisms utilize carbon as an energy source for metabolism, with part of it being released as heat during the composting process.

The carbon utilized by microorganisms during composting primarily originates from starch, lipids, and other simple sugars, as well as a portion of carbon derived from hemicellulose and cellulose, since microbes preferentially decompose the most easily degradable carbon compounds first. In contrast, lignin is the most recalcitrant component of lignocellulosic biomass, making it resistant to microbial breakdown (Wu *et al.* 2022). This intense microbial activity during the early composting stage is believed to be responsible for the initial decrease in carbon content observed in the substrate.

The increase in nitrogen content is attributed to microbial nitrification and nitrogen fixation activities, as well as the relative concentration of nitrogen rising due to the loss of organic matter mass during composting (Azis *et al.* 2023). This phenomenon is consistent with the findings of (Solihat *et al.* 2017), who reported that composting leads to a decrease in the C/N ratio, primarily resulting from the rapid depletion of carbon and the accumulation of total nitrogen in the composting substrate.

The decrease in hydrogen content supports the occurrence of carbohydrate degradation, particularly of cellulose and hemicellulose, which are rich in hydroxyl (-OH) groups. During decomposition, microorganisms break down these compounds into water (H_2O) and volatile gases such as CH_4 or H_2, resulting in the loss of hydrogen in gaseous form (Bernal *et al.* 2009). The reduction in hydrogen content is also associated with an increase in aromatic structures and carbon condensation, as indicated by a decline in the H/C ratio. This decrease in hydrogen during composting consequently reduces the energy potential of the biomass, since hydrogen contributes a higher combustion energy value compared to other elements (Adamovics *et al.* 2018).

3.4 Proximate of Water Hyacinth

Table 4 presents the proximate characteristics of Eichhornia crassipes (*water hyacinth*) during the 15-day composting process. The ash content gradually increased, reaching 32.5% on day 11, while the volatile matter content decreased by 13.34%, and the fixed carbon content increased by 20.25%. These changes were accompanied by an 8.9% reduction in the calorific value, decreasing from 3376.67 cal/g to 3075.67 cal/g. The observed trends indicate progressive mineral accumulation and organic matter loss during composting, reflecting enhanced carbon oxidation and volatilization processes that reduce the energy density of the biomass.

The increase in ash content during the composting process is attributed to the mineralization of organic matter by microorganisms. Microorganisms secrete extracellular hydrolytic enzymes that catalyze the decomposition of organic substrates, leading to the formation of organic-derived minerals. These minerals, produced by decomposer organisms, are water-soluble compounds that can serve as nutrient sources for plants (Bohacz 2019). The accumulation of these minerals contributes to the elevated ash content observed in the composted biomass.

A similar phenomenon was also reported by Chia *et al.* (2022), where the ash content of biomass increased with longer composting duration due to the accumulation of mineral elements such as K, Ca, and Mg, which are not biologically degradable. High ash content is undesirable for fuel applications, as ash consists of non-combustible inorganic components that reduce the calorific value of the material. Moreover, excessive ash formation can lead to the accumulation of solid residues in the combustion chamber, making the system more prone to technical issues such as slagging and fouling, which can impair heat transfer efficiency and damage furnace components.

The decrease in volatile matter (VM) indicates intensive degradation of easily volatile organic compounds, such as hemicellulose, carbonyl compounds, organic acids, and other volatile substances that serve as primary substrates for microbial activity during composting. Chemically, the reduction in VM reflects the transformation of organic materials into more stable compounds, including the formation of fixed carbon structures and an increase in the relative lignin fraction. According to (Meng *et al.* 2021), oxidative reactions during aerobic composting lead to the breakdown of volatile compounds and the formation of humic-like materials that are more resistant to decomposition. The reduction in VM is often associated with a decline in calorific value, as the volatile fraction contributes significantly to the rapid combustion energy of biomass (Díaz *et al.* 2021).

The calorific value of biomass fuel is primarily determined by its fixed carbon (FC) content, which represents the fraction of carbon remaining after the removal of hydrogen, oxygen, nitrogen, and sulfur, and which can withstand high temperatures without volatilization (Sarkar 2015). The fixed carbon content of water hyacinth (WH) during composting showed an increase in the early stages, rising from 13.78% to 16.57% after 11 days. This initial increase in FC is generally attributed to the loss of easily degradable fractions such as hemicellulose, cellulose, and volatile compounds during microbial decomposition, leading to the relative enrichment of more stable carbon components like lignin (Wang *et al.* 2021).

However, at the end of the composting period, the fixed carbon (FC) content decreased again, indicating that once most of the easily degradable materials had been exhausted, microorganisms began decomposing the more resistant lignocellulosic fractions. Lignin, which is initially relatively stable, can undergo partial depolymerization due to the activity of ligninase enzymes produced by certain fungi and bacteria. As a result, the solid carbon content slightly decreased because a portion of the lignin was converted into simpler organic compounds and gaseous products through microbial respiration.

Table 4
Proximate of water hyacinth after composting (0, 4, 7, 11, and 15).

Proximate	Composting time (days)				
	0	4	7	11	15
Ash Content (%)	16.6011[a]	18.1178[b]	18.7858[c]	21.9993[e]	21.3364[d]
Volatile Matter (%)	60.0364[d]	56.3724[c]	54.9652[b]	52.0294[a]	54.5693[b]
Fixed Carbon (%)	13.7824 [a]	15.3717 [b]	15.9034 [b]	16.5738 [b]	13.9515 [a]
Caloric value (cal/g)	3376.67 [d]	3217.67 [c]	3177.67 [bc]	3075.67 [ab]	3041.00 [a]

* Treatment values followed by different letters indicate a significant difference at the 5% level

Table 5
Proximate test results on water hyacinth after demineralization

Proximate	Composting time (days)				
	0	4	7	11	15
Demineralization with water					
Ash Content (%)	10.8373^{b}	12.2363^{cd}	10.1327^{a}	11.8422^{c}	12.3594^{d}
Volatile Matter (%)	64.2469^{b}	62.8245^{a}	63.0394^{b}	62.0012^{a}	62.5719^{a}
Fixed Carbon (%)	16.6766^{a}	18.1430^{a}	17.3345^{b}	16.4686^{b}	16.5136^{a}
Caloric value (cal/g)	3741.29^{c}	3542.93^{a}	3658.37^{b}	3515.08^{a}	3703.98^{a}
Demineralization with HNO_3 5%					
Ash Content (%)	3.5377^{a}	4.3169^{b}	4.6194^{c}	5.4176^{d}	6.5693^{e}
Volatile Matter (%)	68.1608c	67.8276^{c}	66.2797^{b}	65.1271^{ab}	64.0540^{a}
Fixed Carbon (%)	20.9282^{a}	22.8159^{a}	22.5624^{a}	21.1491^{a}	20.9709^{a}
Caloric value (cal/g)	4195.95^{b}	4037.25^{ab}	4016.75^{ab}	3939.86^{a}	3974.75^{ab}

* Treatment values followed by different letters indicate a significant difference at the 5% level

From an energy perspective, the temporary increase in fixed carbon (FC) during the early stages of composting reflects a relative enrichment of carbon, which can potentially enhance the calorific value of the biomass. However, since the composting process as a whole promotes oxidation and the loss of organic carbon, this effect is temporary. It is eventually followed by a decline in calorific value at the later stages of composting.

3.5 Demineralization of Water Hyacinth

Demineralization is needed to reduce the high ash content of WH due to composting. Table 5 displays the washing outcomes of WH without composting and WH with a water solvent and a 5% concentration of nitric acid (HNO_3), following the use of water for washing. The amount of WH ash without composting reduced from 16.6% to 10.84%. This represents a loss of 34.7%. This finding aligns with research (Zouari *et al.* 2024), which demonstrated that rinsing olive stones with water can decrease ash content by 40%. Post-composting washing of the raw material can effectively minimize ash content in comparison to pre-composting washing. The reason for this is that the breakdown of organic matter leads to the formation of a less compact and more porous structure. Additionally, certain inorganic minerals might transform into more soluble compounds during the composting process, which facilitates their removal by washing (Zhang *et al.* 2020).

Following the composting of WH. there was a substantial rise in the reduction of ash levels. The most dramatic decrease in 11 days was seen with ash levels dropping from 22% to 11.84% (a decrease of 46.17%). This occurrence did not transpire while cleansing with a solution containing 5% nitric acid. When using a 5% concentration of nitric acid for washing. The WH sample without composting showed the most significant decrease in ash levels. Reaching 3.53% (78.69%).

Nevertheless, during the process of constructing WH. The duration of the composting period resulted in a reduction in the ash content after washing. The ash levels decreased sequentially from 76.17% to 75.41%, then to 75.37%, and finally to 69.21%. The composting process involves the conversion of organic waste into humic acid. A chemical that progressively accumulates over time. Humic acid is formed from the breakdown of organic matter that is not soluble in acid (Mindari *et al.* 2022). The decrease in the presentation of ash washing results when using 5% nitric acid can be attributed to the solubility of humic acid in water. Humic acid is a hydrophilic colloid with a strong affinity for water. Making washing with water of pH 7 more effective. This is because some of the humic acid dissolves in water. Resulting in improved washing results (Ariyanto DP 2006).

The volatile matter (VM) content in samples washed with water increased by 19.17%, and by 25.17% in those treated with acid, indicating that the removal of minerals did not damage the volatile organic fractions such as hemicellulose and light carbon compounds. This finding is consistent with Singhal *et al.* (2021), who reported that water washing can increase VM content due to the removal of non-volatile inorganic components. In addition, the fixed carbon (FC) content increased by 18.36%, suggesting that the reduction in ash content led to a relative increase in the proportion of solid carbon within the total biomass mass.

3.6 Energy Yield and Combustion Characteristics

The calorific value of biomass reflects the amount of energy released during combustion. Table 4 shows that the heating value of water hyacinth gradually decreased from 3376.67 cal/g to 3041.00 cal/g throughout the composting process. This reduction corresponds with the decline in volatile matter and the increase in ash content. The volatile fraction contains high levels of carbon and hydrogen; thus, a decrease in VM directly results in lower combustion energy (Parikh *et al.* 2005). Moreover, the increase in non-combustible ash content further reduces the energy density of the material (Liu *et al.* 2024). After water demineralization, the heating value increased by 18%, indicating that water washing effectively improves the energy quality of the biomass. This process enhances the relative fraction of organic carbon with respect to the total dry mass (Sommersacher *et al.* 2015). Demineralization treatment with 5% HNO_3 resulted in a significant increase of up to 50%, indicating the high efficiency of nitric acid in dissolving alkali and alkaline earth metals (K, Na, Ca, Mg, Fe). This leaching process also enriches the fixed carbon fraction, which possesses a higher heating value compared to the volatile fraction.

Overall, these results indicate that demineralization—particularly with nitric acid—effectively enhances the calorific value of Eichhornia crassipes by removing non-combustible inorganic minerals and enriching the organic carbon fraction. The acid-demineralized biomass exhibits more stable energy characteristics and demonstrates strong potential as a high-quality solid fuel.

3.7 Correlation Between Structural Carbohydrate Fractions and Thermochemical Characteristics of Biomass

The composting process led to a reduction in cellulose and hemicellulose due to microbial degradation. The decline in these carbohydrate fractions affected the lignin content, proximate composition, ultimate analysis, and calorific value of the biomass. The correlations among these components are

Table. 6
Correlation between elements

		Lignin	Ash	Carbon (C)	Caloric Value	Cellulose	Hemicellulose	Volatile matter	Fixed Carbon	Hydrogen (H)	Nitrogen (N)	Sulfur (S)	Oxygen (O)
Lignin	Pearson Correlation	1	.909**	-.842**	-.832**	-.921**	-.907**	-.813**	.225	-.842**	-.796**	.591*	.877**
	Sig. (2-tailed)		.000	.000	.000	.000	.000	.000	.420	.000	.000	.020	.000
Ash	Pearson Correlation	.909**	1	-.809**	-.878**	-.841**	-.923**	-.892**	.331	-.809**	-.811**	.559*	.789**
	Sig. (2-tailed)	.000		.000	.000	.000	.000	.000	.228	.000	.000	.030	.000
Carbon (C)	Pearson Correlation	-.842**	-.809**	1	.719**	.822**	.907**	.853**	-.419	1.000**	.823**	-.507	-.623*
	Sig. (2-tailed)	.000	.000		.003	.000	.000	.000	.120	0.000	.000	.054	.013
Caloric Value	Pearson Correlation	-.832**	-.878**	.719**	1	.868**	.906**	.806**	-.265	.719**	.733**	-.687**	-.639*
	Sig. (2-tailed)	.000	.000	.003		.000	.000	.000	.341	.003	.002	.005	.010
Cellulose	Pearson Correlation	-.921**	-.841**	.822**	.868**	1	.902**	.748**	-.108	.822**	.769**	-.592*	-.745**
	Sig. (2-tailed)	.000	.000	.000	.000		.000	.001	.702	.000	.001	.020	.001
Hemicellulose	Pearson Correlation	-.907**	-.923**	.907**	.906**	.902**	1	.913**	-.408	.907**	.846**	-.695**	-.672**
	Sig. (2-tailed)	.000	.000	.000	.000	.000		.000	.131	.000	.000	.004	.006
Volatile matter	Pearson Correlation	-.813**	-.892**	.853**	.806**	.748**	.913**	1	-.680**	.853**	.813**	-.581*	-.560*
	Sig. (2-tailed)	.000	.000	.000	.000	.001	.000		.005	.000	.000	.023	.030
Fixed Carbon	Pearson Correlation	.225	.331	-.419	-.265	-.108	-.408	-.680**	1	-.419	-.470	.311	-.069
	Sig. (2-tailed)	.420	.228	.120	.341	.702	.131	.005		.120	.077	.259	.808
Hydrogen (H)	Pearson Correlation	-.842**	-.809**	1.000**	.719**	.822**	.907**	.853**	-.419	1	.823**	-.507	-.623*
	Sig. (2-tailed)	.000	.000	0.000	.003	.000	.000	.000	.120		.000	.054	.013
Nitrogen (N)	Pearson Correlation	-.796**	-.811**	.823**	.733**	.769**	.846**	.813**	-.470	.823**	1	-.453	-.538*
	Sig. (2-tailed)	.000	.000	.000	.002	.001	.000	.000	.077	.000		.090	.039
Sulfur (S)	Pearson Correlation	.591*	.559*	-.507	-.687**	-.592*	-.695**	-.581*	.311	-.507	-.453	1	.472
	Sig. (2-tailed)	.020	.030	.054	.005	.020	.004	.023	.259	.054	.090		.076
Oxygen (O)	Pearson Correlation	.877**	.789**	-.623*	-.639*	-.745**	-.672**	-.560*	-.069	-.623*	-.538*	.472	1
	Sig. (2-tailed)	.000	.000	.013	.010	.001	.006	.030	.808	.013	.039	.076	

**. Correlation is significant at the 0.01 level (2-tailed).
*. Correlation is significant at the 0.05 level (2-tailed).

presented in Table 6. Cellulose exhibited a strong positive correlation with carbon content (0.822), calorific value (0.868), volatile matter (0.748), and nitrogen content (0.769), while showing a negative correlation with lignin (-0.921), ash content (-0.841), and oxygen (-0.745). Similarly, hemicellulose showed comparable correlation patterns to cellulose, indicating that the

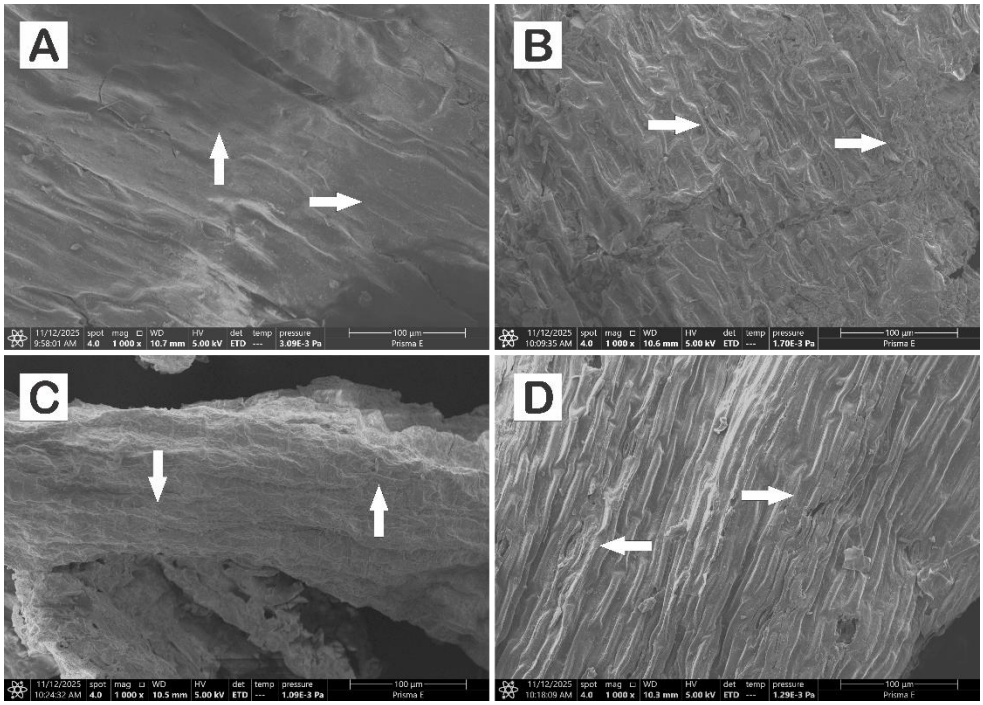

Fig.2. SEM micrographs of water hyacinth: untreated sample (A), sample after 11 days of composting (B), composted sample (11 days) followed by demineralization with distilled water (C), and composted sample (11 days) followed by demineralization with 5% nitric acid (D). The white arrows indicate the nano-sized cracks. Magnification: 1000×.

reduction of polysaccharide components plays a crucial role in determining both the chemical composition and energy characteristics of the composted biomass.

This positive correlation indicates that the reduction of structural carbohydrate fractions (cellulose and hemicellulose) plays a crucial role in the decline of volatile components and the overall energy content of the biomass. Moreover, the depletion of these carbohydrates is associated with an increase in lignin, ash, and oxygen contents. The decrease in cellulose typically leads to a reduction in volatile matter (VM), as this component readily decomposes into gases and organic vapors during thermal treatment. Overall, these findings suggest that the degradation of cellulose and hemicellulose exerts a dominant influence on the thermochemical characteristics and energy potential of solid biofuels derived from biomass.

3.8 Surface Morphological Characterization of the Material

Aerobic composting and demineralization treatments influenced the ultrastructure of the water hyacinth material, as shown in Figure 2. The untreated sample exhibited a smooth surface with no visible cracks (Figure 2A). Surface cracks began to appear after 11 days of composting, indicating degradation of structural carbohydrate components. Cracks remained visible in the sample demineralized with distilled water (Figure 2C), and the surface appeared more wrinkled, likely due to the reduction of alkaline and alkaline earth minerals.

The sample demineralized with nitric acid exhibited a fragile surface with more pronounced cracking. These cracks were likely caused by the removal of minerals and the degradation of holocellulose, particularly hemicellulose, as discussed in the demineralization section. According to Jiang *et al.* (2013) and Asadieraghi and Wan Daud (2014), acid-based demineralization can alter the morphological structure of biomass, often resulting in an eroded appearance. This effect may arise from the removal of minerals, extractives, and holocellulose.

3.9 XRD Analysis

Figure 3 shows the X-ray diffraction (XRD) spectra of four different treatments applied to the raw materials. X-ray diffraction (XRD) is able to explain the crystalline phase of the raw materials (Liao *et al.* 2016). After 11 days of composting (E3), the crystallinity of the raw materials grew from 32.79% to 33.88% (Table 7). The increase in crystallinity observed in E3 compared to E0 indicates that the aerobic composting process for 11 days led to the degradation of amorphous components such as hemicellulose and lignin, thereby increasing the relative proportion of crystalline cellulose.

Demineralization treatments using water (DWE3) and nitric acid (DAE3) significantly reduced the crystallinity of the biomass. This reduction indicates that washing and acid treatments facilitate the removal of alkali and alkaline earth metal ions (K, Na, Ca, Mg) and promote the degradation of

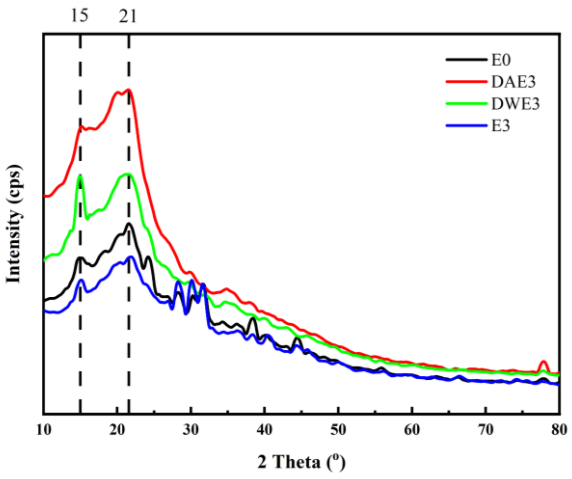

Fig. 3. XRD pattern of water hyacinth sample after composting

Table 7
XRD pattern of water hyacinth sample after composting

Sample	Crystallinity (%)	Crystal Icr (kcps*deg)	Amorphous Ia (kcps*deg)
E0	32.78	1.94	3.98
DAE3	17.85	1.07	4.95
DAWE3	22.58	1.31	4.50
E3	33.87	1.54	3.00

crystalline cellulose structures through the hydrolysis of glycosidic bonds. The oxidative nature of nitric acid can also attack β-1,4-glycosidic linkages, thereby expanding the amorphous regions within the cellulose matrix (Li *et al.* 2021). Consequently, the cellulose structure becomes more disordered, resulting in a substantial decrease in crystallinity, particularly in the DAE3 sample (17.85%).

This high crystallinity can be attributed to the presence of ash-forming minerals in the raw materials. Ash-forming minerals included in biomass consist of organic and inorganic minerals, which show varying degrees of crystallinity (Vassilev *et al.* 2013). Crystallinity is influenced by the chemical composition of the raw materials such as cellulose, hemicellulose, and lignin. The degradation of amorphous cellulose during the composting process results in an increase in the amount of crystalline cellulose. Crystallinity decreased to 22.59% after washing with water (DWE 3) and was the lowest in the washing treatment using 5% nitric acid (DAE 3), which was 17.85%. This decrease in crystallinity indicates a decrease in ash content, which is also caused by the degradation of crystalline cellulose due to washing.

3.10 FTIR Analysis

Fourier Transform Infrared (FTIR) spectroscopy analysis was conducted to identify changes in functional groups and absorption intensities after composting and mineral leaching (Figure 4). The FTIR spectra in Figure 4 exhibit the characteristic absorption bands of lignocellulosic biomass and show notable alterations after composting (E3) and demineralization (DWE3 and DAE3). The broad absorption band around 3300 cm^{-1} corresponds to the O–H stretching region of hydroxyl groups present in cellulose, hemicellulose, and lignin (Solihat *et al.* 2017). The increased intensity of this band in DWE3 and DAE3 samples indicates greater exposure

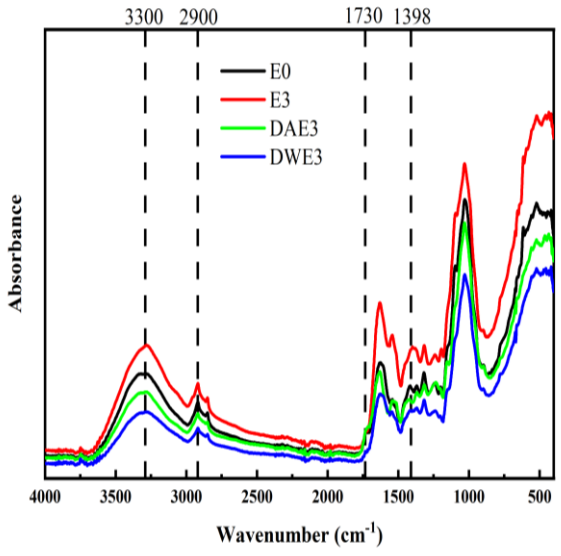

Fig. 4. FTIR spectrum of composted water hyacinth

of hydroxyl groups due to mineral removal and structural degradation during treatment. The band near 2900 cm^{-1}, associated with aliphatic C–H stretching, remains visible across all samples, suggesting that the main hydrocarbon backbone was preserved. In contrast, the decreased intensity of the 1730 cm^{-1} band (C=O stretching in acetyl groups of hemicellulose) observed in E3 and further reduced in DWE3 and DAE3 indicates hydrolysis or leaching of hemicellulosic fractions as a result of microbial activity and acid treatment.

An absorption difference was detected at a wavenumber of 1542 cm^{-1}. This was evident in the compounds E3 and DAE3. The peak observed at around 1542 cm^{-1} is a result of the stretching vibration of the C=C double bond within the aromatic ring. Furthermore, this vibration is associated with the distortions of the aromatic ring in lignin (Duan *et al.* 2022). This validates the increase in lignin concentration after demineralization with water, in accordance with the results of the lignin test, which increased from 10.57% (E0) to 13.51% (DWE3) as acid removes lignin. The post-demineralised material. Which exhibits a peak at 1542 cm^{-1} in the HNO_3 spectrum. Undergoes shrinkage. The presence of a peak at 1542 cm^{-1} indicates that washing with water is ineffective in removing lignin. The hemicellulose shows another distinction at a peak of 1398 cm^{-1}. This is linked to the flexing movement of the C-H bond in the methyl group (Kostryukov *et al.* 2023). This validates the existence of bacterial and fungal activity during the composting process, which is responsible for the early breakdown of the hemicellulose.

The band around 1260 cm^{-1} (C–O stretching in guaiacyl/syringyl lignin units) exhibited a noticeable increase in intensity after treatment, reinforcing the indication of lignin accumulation. Conversely, the band at 1050–1030 cm^{-1}, attributed to C–O and C–O–C stretching vibrations in cellulose and hemicellulose, showed a marked decrease in intensity in DWE3 and DAE3 samples, suggesting polysaccharide dissolution or a reduction in the crystalline fraction. This trend is further supported by the XRD results, where the crystallinity index significantly decreased, particularly in DAE3 (17.85%), indicating that acid treatment disrupted the ordered cellulose structure and enhanced the amorphous character of the biomass. Overall, the FTIR findings confirm that composting and demineralization induced selective degradation of amorphous components such as hemicellulose and cellulose, while lignin remained relatively stable and accumulated proportionally.

The structural changes detected by XRD and FTIR closely correlate with the measured fuel properties. Based on the XRD results, the crystallinity index decreased from 32.79% in E0 to 17.85% in DAE3, indicating an increase in the amorphous fraction. The FTIR spectra support this observation, showing a relative decline in bands associated with polysaccharides (1030–1050 cm^{-1}) and a reduction in the hemicellulose carbonyl/ester band (1730 cm^{-1}), accompanied by an intensified aromatic lignin signal around 1510 cm^{-1}. This compositional transformation is reflected in the fuel characteristics. Although the relative lignin content increased, the higher proportion of amorphous and oxygenated structures resulted in an overall decrease in calorific value.

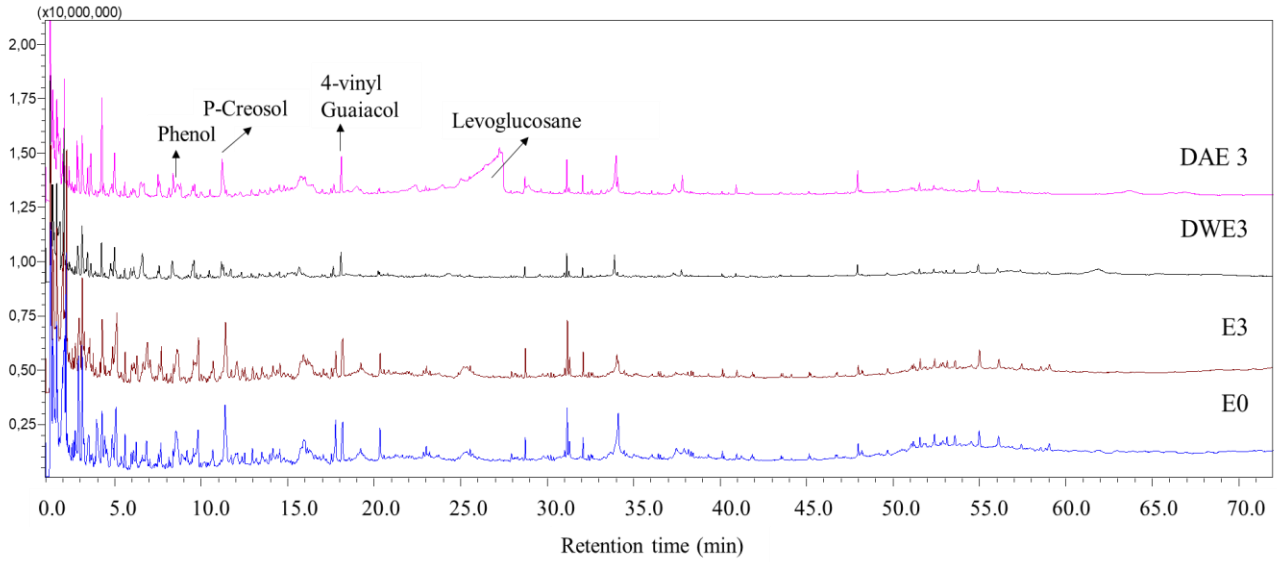

Fig. 5. Pyrogram of sample untreated (E0) and treated ones (E3. DWE3. and DAE3)

The decrease in calorific value can be quantitatively explained by two primary factors revealed through spectroscopic and diffraction data. First, the loss of combustible carbon-rich polysaccharide fractions—evidenced by the reduction in FTIR band intensities at 1030–1050 cm^{-1} and 1730 cm^{-1}—resulted in a decline in total carbon content from 36.43% to 33.75%. Second, the increase in the non-combustible ash fraction exhibited a strong negative correlation with the calorific value (R^2 = 0.77). In other words, the reduction in crystallinity reflects the degradation and release of carbohydrate structures into CO_2 and volatile compounds, as indicated by the diminished polysaccharide absorption bands in the FTIR spectra. Although the relative proportion of lignin increased, the total amount of carbon contributing to combustion energy decreased, while ash content increased—ultimately reducing the overall energy density of the biomass.

3.11 PyGC-MS analysis

Rapid analysis of lignocellulose derivatives from the sample control (untreated) and treated is shown in Figure 5. 67 peaks of pyrolysis products from lignocellulose, such as extractives. Carbohydrates and lignin were detected from the samples (Ismayati *et al.* 2016). Lignin derivatives were detected as phenol. P-creosol and 4-vinyl guaiacol, then the typical levoglucosan peak was found at a retention time of 27.4 minutes (Ismayati *et al.* 2016). Total derivatives of lignin were 4.28%. 7.31%. 4.96% and 5.22% for E0. E3. DWE3. and DAE3. respectedly. These results have supported the data shown by FTIR where the composting process has succeeded in increasing the amount of lignin compared to the control.

4. Conclusions

Water hyacinth biomass quality as a solid fuel was successfully improved through controlled composting and post-composting demineralization. Composting for 15 days increased the relative lignin content from 10.01% to 15.14% due to selective degradation of cellulose and hemicellulose, while the most effective ash reduction (46.17%) occurred when 11-day composted biomass was washed, lowering ash from 22% to 11.84%. Demineralization after composting was more effective than before composting, as microbial decomposition enhanced porosity and mineral solubility.

Water washing preserved thermochemical integrity better than 5% HNO_3, which caused partial lignin and cellulose depolymerization, reducing crystallinity to 17.85%. Structural analyses (SEM, FTIR, XRD, and PyGC-MS) consistently confirmed polysaccharide loss, lignin accumulation, and mineral removal effects. Overall, treated water hyacinth shows strong potential as a sustainable solid fuel feedstock due to higher lignin proportion, significantly reduced ash, and improved fixed-carbon enrichment, despite a moderate decline in raw calorific value during composting.

.

Acknowledgments

This author expresses thanks to the Central Java Provincial Government of the Republic of Indonesia, RIIM LPDP Grant and BRIN (B-3838/II.7.5/FR.06.00/11/2023), and the Research Organization for Nanotechnology and Materials-National Research and Innovation Agency (BRIN) research grant 2025.

Author Contributions: Mustaghfirin Mustaghfirin: Investigation, data curation, writing-original draft preparation, and visualization. Dede Hermawan: supervision, conceptualization, writing, review, and editing. Deded Sarip Nawawi: supervision, conceptualization, writing, review, and editing. Sukma Surya Kusumah: supervision, conceptualization, writing, review, and editing. Maya Ismayati: formal analysis, writing, review, and editing. Jajang Sutiawan: formal analysis, writing, review, and editing. Riska Surya Ningrum: formal analysis, writing, review, and editing.

Funding: This research was funded by the Central Java Provincial Government of the Republic of Indonesia, RIIM LPDP Grant and BRIN (B-3838/II.7.5/FR.06.00/11/2023), and the Research Organization for Nanotechnology and Materials-National Research and Innovation Agency (BRIN) research grant 2025.

Conflicts of Interest: The authors declare no conflict of interest.

References

Adamovics, A., Platace, R., Gulbe, I., and Ivanovs, S. (2018). The content of carbon and hydrogen in grass biomass and its influence on heating value. *Engineering for Rural Development*. https://doi.org/10.22616/ERDev2018.17.N014

Agung A. (2016). Aktivitas Proses Dekomposisi Berbagai Bahan Organik Dengan Aktivator Alami dan Buatan, *Jurnal Ilmu Pertanian 13 (2), 92-104*

Ahamer, G. (2022). Why Biomass Fuels Are Principally Not Carbon Neutral, *Energies*, 15(24). https://doi.org/10.3390/en15249619

Ariyanto DP. (2006). Ikatan Antara Asam Organik Tanah dengan Logam, Karya Ilmiah Pasca Sarjana Ilmu Tanah. Yogyakarta: Universitas Gadjah Mada, 1–13.

Azis, F. A., Choo, M., Suhaimi, H., and Abas, P. E. (2023). The Effect of Initial Carbon to Nitrogen Ratio on Kitchen Waste Composting Maturity, *Sustainability (Switzerland)*, 15(7). https://doi.org/10.3390/su15076191

Barneto, A. G., Carmona, J. A., Gálvez, A., and Conesa, J. A. (2009). Effects of the composting and the heating rate on biomass gasification. *Energy and Fuels*, 23(2), 951–957. https://doi.org/10.1021/ef8005806

Bernal, M. P., Alburquerque, J. A., and Moral, R. (2009). Composting of animal manures and chemical criteria for compost maturity assessment. A review. *Bioresource Technology*, 100(22). https://doi.org/10.1016/j.biortech.2008.11.027

Bohacz, J. (2019). Changes in mineral forms of nitrogen and sulfur and enzymatic activities during composting of lignocellulosic waste and chicken feathers. *Environmental Science and Pollution Research*, 26(10). https://doi.org/10.1007/s11356-019-04453-2

Chia, W. Y., Chew, K. W., Le, C. F., Chee, C. S. C., Ooi, M. S. L., and Show, P. L. (2022). Utilization of Aerobic Compression Composting Technology on Raw Mushroom Waste for Bioenergy Pellets Production. *Processes*, 10(3). https://doi.org/10.3390/pr10030463

Darmawan, S. A. C., R., Sihombing, A. L., and Cendrawati, D. G. (2021). Potential and Characteristics of Eichhornia Crassipes Biomass and Municipal Solid Waste As Raw Materials for RDF in Co-Firing Coal Power Plants, *IOP Conference Series: Earth and Environmental Science*, 926(1). https://doi.org/10.1088/1755-1315/926/1/012009

Díaz, M. J., Ruiz-Montoya, M., Palma, A., and de-Paz, M. V. (2021). Thermogravimetry applicability in compost and composting research: A review. *Applied Sciences (Switzerland)*, 11(4). https://doi.org/10.3390/app11041692

Duan, J., Huang, R. J., Gu, Y., Lin, C., Zhong, H., Xu, W., Liu, Q., You, Y., Ovadnevaite, J., Ceburnis, D., Hoffmann, T., and O'Dowd, C. (2022). Measurement report: Large contribution of biomass burning and aqueous-phase processes to the wintertime secondary organic aerosol formation in Xi'an, Northwest China. *Atmospheric Chemistry and Physics*, 22(15), 10139–10153. https://doi.org/10.5194/acp-22-10139-2022

Esteves, B., Sen, U., and Pereira, H. (2023). Influence of Chemical Composition on Heating Value of Biomass: A Review and Bibliometric Analysis, *Energies*, 16(10), 1–17. https://doi.org/10.3390/en16104226

Hemida, M. H., Moustafa, H., Mehanny, S., Morsy, M., Abd EL Rahman, E. N., and Ibrahim, M. M. (2024). Valorization of Eichhornia crassipes for the production of cellulose nanocrystals further investigation of plethoric biobased resource, *Scientific Reports*, 14(1), 12387. https://doi.org/10.1038/s41598-024-62159-z

Huang, L., Xie, C., Liu, J., Zhang, X., Chang, K. L., Kuo, J., Sun, J., Xie, W., Zheng, L., Sun, S., Buyukada, M., and Evrendilek, F. (2018). "Influence of catalysts on co-combustion of sewage sludge and water hyacinth blends as determined by TG-MS analysis," *Bioresource Technology*, Elsevier, 247(September 2017), 217–225. https://doi.org/10.1016/j.biortech.2017.09.039

Hudakorn, T., and Sritrakul, N. (2020). Biogas and biomass pellet production from water hyacinth, *Energy Reports*, Elsevier Ltd, 6, 532–538. https://doi.org/10.1016/j.egyr.2019.11.115

Ismayati, M., Nakagawa-Izumi, A., Kamaluddin, N. N., and Ohi, H. (2016). Toxicity and feeding deterrent effect of 2-methylanthraquinone from thewood extractives of Tectona grandis on the subterranean termites Coptotermes formosanus and Reticulitermes speratus. *Insects*, 7(4). https://doi.org/10.3390/insects7040063

Jiang, L., Hu, S., Sun, L. shi, Su, S., Xu, K., He, L. mo, and Xiang, J. (2013). Influence of different demineralization treatments on physicochemical structure and thermal degradation of biomass. *Bioresource Technology*, 146, 254–260. https://doi.org/10.1016/j.biortech.2013.07.063

Kementerian, and ESDM. (2024). Hingga 2030, Permintaan Energi Dunia Meningkat 45 %, *Kementerian ESDM RI*, 1–3.

Kostryukov, S. G., Matyakubov, H. B., Masterova, Y. Y., Kozlov, A. S., Pryanichnikova, M. K., Pynenkov, A. A., and Khluchina, N. A. (2023). Determination of Lignin, Cellulose, and Hemicellulose in Plant Materials by FTIR Spectroscopy. *Journal of Analytical Chemistry*, 78(6), 718–727. https://doi.org/10.1134/S1061934823040093

Krzywanski, J., Czakiert, T., Zylka, A., Nowak, W., Sosnowski, M., Grabowska, K., Skrobek, D., Sztekler, K., Kulakowska, A., Ashraf, W. M., and Gao, Y. (2022). Modelling of SO2 and NOx Emissions from Coal and Biomass Combustion in Air-Firing, Oxyfuel, iG-CLC, and CLOU Conditions by Fuzzy Logic Approach, *Energies*, 15(21). https://doi.org/10.3390/en15218095

Kukuruzović, J., Matin, A., Kontek, M., Krička, T., Matin, B., Brandić, I., and Antonović, A. (2023). The Effects of Demineralization on Reducing Ash Content in Corn and Soy Biomass with the Goal of Increasing Biofuel Quality, *Energies*, 16(2). https://doi.org/10.3390/en16020967

Li, F., He, X., Srishti, A., Song, S., Tan, H. T. W., Sweeney, D. J., Ghosh, S., and Wang, C. H. (2021). Water hyacinth for energy and environmental applications: A review, *Bioresource Technology*. https://doi.org/10.1016/j.biortech.2021.124809

Liang, D., Chen, Y., Zhu, S., Gao, Y., Sun, T., Ri, K., and Xie, X. (2021). Low-temperature conversion of Fe-rich sludge to KFeS2 whisker: a new flocculant synthesis from laboratory scale to pilot scale. *Sustainable Environment Research*, 31(1). https://doi.org/10.1186/s42834-021-00098-4

Liao, R., Xu, J., and Umemura, K. (2016). Low Density Sugarcane Bagasse Particleboard Bonded with Citric Acid and Sucrose: Effect of board density and additive content, *BioResources*, 11(1). https://doi.org/10.15376/BIORES.11.1.2174-2185

Liu, C., Qiu, T., Cao, W., Liu, H., Zhao, W., Mostafa, E., and Zhang, Y. (2024). Water-washing treatment can change biochar microstructure: microwave pyrolysis of biomass, *Energy Sources, Part A: Recovery, Utilization and Environmental Effects*, 46(1). https://doi.org/10.1080/15567036.2024.2302010

Meng, J., Zhang, X., Ai, Y., Yue, H., Li, X., and Chen, R. (2021). Deslagging of Eichhornia crassipers and Pistia stratiotes biomass pellets, *Energy Reports*, 7. https://doi.org/10.1016/j.egyr.2021.01.010

Mindari, W., Sassongko, P. E., and Syekhfani. (2022). *Asam Humat*.Edisi 3, UPN Jawa Timur, https://repository.upnjatim.ac.id/4125/1/Asam_humat_edisi%203.pdf

Murda, R. A., Maulana, S., Fatrawana, A., Mangurai, S. U. N. M., Muhamad, S., Hidayat, W., and Bindar, Y. (2022). Changes in Chemical Composition of Betung Bamboo (Dendrocalamus asper) after Alkali Immersion Treatment under Various Immersion Times, *Jurnal Sylva Lestari*, 10(3), 358–371. https://doiorg/10.23960/jsl.v10i3.599

Mustamu, S., and Pari, G. (2018). Kharateristik biopellet dari limbah padat kayu putih dan gondorukem, *Jurnal Penelitian Hasil Hutan*, 36(3), 191–204. https://doi.org/10.20886/jphh.2018.36.3.191-204

Nawawi, D. S., Carolina, A., Saskia, T., Darmawan, D., Gusvina, S. L., Wistara, N. J., Sari, R. K., and Syafii, W. (2018). Chemical Characteristics of Biomass for Energy, *J. Ilmu Teknol. Kayu Tropis*, 16(1), 44–51.

Parikh, J., Channiwala, S. A., and Ghosal, G. K. (2005). A correlation for calculating HHV from proximate analysis of solid fuels, *Fuel*, 84(5), 487–494. https://doi.org/10.1016/j.fuel.2004.10.010

Peraturan, P. M., Republik, P., Nomor, I., Presiden, P., and Indonesia, R. (2006). Perpres Nomar 5 Tahun2006 : Kebijakan Energi Nasional,1–5.

Putri, M. I. D. W., Murda, R. A., Maulana, S., Octaviani, E. A., Sari, N. A., Hasibuan, M. M., Aulia, F., and Hidayat, W. (2024). Hybrid

Biopellets Characterization of Gamal Wood (Gliricidia sepium) and Robusta Coffee Husk at Various Compositions, *Jurnal Sylva Lestari*, 12(3), 595–609. https://doi.org/10.23960/jsl.v12i3.913

Ratih, Y. W., Sohilait, D. A., and Widodo, R. A. (2018). Uji aktivitas dekomposisi dari beberapa inokulum komersial pada berbagai jenis bahan berdasarkan jumlah CO2 yang terbentuk. *Jurnal Tanah dan Air,* 15(2), 93–102. https://doi.org/10.31315/jta.v15i2.4004

Saputra, N. A., Darmawan, S., Efiyanti, L., Hendra, D., Wibowo, S., Santoso, A., Djarwanto, Gusmailina, Komarayati, S., Indrawan, D. A., Yuniawati, Nawawi, D. S., Maddu, A., Pari, G., and Syafii, W. (2022). A Novel Mesoporous Activated Carbon Derived from Calliandra calothyrsus via Physical Activation: Saturation and Superheated. *Energies*, 15(18). https://doi.org/10.3390/en15186675

Sarkar, D. K. (2015). .Chapter 3 - Fuels and Combustion. D. K. B. T.-T. P. P. Sarkar, ed., Elsevier, 91–137. DOI: https://doi.org/10.1016/B978-0-12-801575-9.00003-2

Singhal, A., Goossens, M., Konttinen, J., and Joronen, T. (2021). Effect of basic washing parameters on the chemical composition of empty fruit bunches during washing pretreatment: A detailed experimental, pilot, and kinetic study, *Bioresource Technology*, 340. https://doi.org/10.1016/j.biortech.2021.125734

Solihat, N. N., Sari, F. P., Risanto, L., Anita, S. H., Fitria, Fatriasari, W., and Hermiati, E. (2017). Disruption of oil palm empty fruit bunches by microwave-assisted oxalic acid pretreatment, *Journal of Mathematical and Fundamental Sciences*, 49(3). https://doi.org/10.5614/j.math.fund.sci.2017.49.3.3

Sommersacher, P., Kienzl, N., Brunner, T., and Obernberger, I. (2015). Simultaneous Online Determination of S, Cl, K, Na, Zn, and Pb Release from a Single Particle during Biomass Combustion. Part 1: Experimental Setup-Implementation and Evaluation. *Energy and Fuels*, 29(10). https://doi.org/10.1021/acs.energyfuels.5b00621

Tuomela, M., Vikman, M., Hatakka, A., and Itävaara, M. (2000). Biodegradation of lignin in a compost environment: A review, *Bioresource Technology*, 72(2). https://doi.org/10.1016/S0960-8524(99)00104-2

Usino, D. O., Sar, T., Ylitervo, P., and Richards, T. (2023). Effect of Acid Pretreatment on the Primary Products of Biomass Fast Pyrolysis, *Energies*, 16(5). https://doi.org/10.3390/en16052377

Vassilev, S. V., Baxter, D., Andersen, L. K., and Vassileva, C. G. (2013). An overview of the composition and application of biomass ash. Part 1. Phase-mineral and chemical composition and classification. *Fuel*, Elsevier Ltd, 105, 40–76. https://doi.org/10.1016/j.fuel.2012.09.041

Velázquez-Araque, L., Muñoz Cajiao, C., Solis-Cordero, E., and Vásquez-Inca, G. (2020). Eichhornia crassipes: A new energy source for biopellets production. *European Biomass Conference and Exhibition Proceedings*, (September), 377–383. https://doi.org/10.5071/28thEUBCE2020-2BV.2.43

Wang, S., Zou, C., Yang, H., Lou, C., Cheng, S., Peng, C., Wang, C., and Zou, H. (2021). Effects of cellulose, hemicellulose, and lignin on the combustion behaviours of biomass under various oxygen concentrations. *Bioresource Technology*, 320. https://doi.org/10.1016/j.biortech.2020.124375

Wichianphong N and Maison W. (2020). Preparation of biofuel pellets from water hyacinth and waste coffee grounds. *RMUTSB Acad. J.*, 8(2), 140–152. https://li01.tci-thaijo.org/index.php/rmutsb-sci/article/view/247484

Wistara, N. J., Bahri, S., and Pari, G. (2020). Biopellet properties of agathis wood fortified with its peeled-off bark, *IOP Conference Series: Materials Science and Engineering*, 935(1). https://doi.org/10.1088/1757-899X/935/1/012047

Wu, D., Wei, Z., Mohamed, T. A., Zheng, G., Qu, F., Wang, F., Zhao, Y., and Song, C. (2022). Lignocellulose biomass bioconversion during composting: Mechanism of action of lignocellulase, pretreatment methods and future perspectives. *Chemosphere*, 286. https://doi.org/10.1016/j.chemosphere.2021.131635

Yang, H., Zhang, H., Qiu, H., Anning, D. K., Li, M., Wang, Y., and Zhang, C. (2021). Effects of C/N ratio on lignocellulose degradation and enzyme activities in aerobic composting, *Horticulturae*, 7(11), 1–13. https://doi.org/10.3390/horticulturae7110482

Zhang, C., Ma, X., Zheng, C., Huang, T., Lu, X., and Tian, Y. (2020). Co-hydrothermal Carbonization of Water Hyacinth and Sewage Sludge: Effects of Aqueous Phase Recirculation on the Characteristics of Hydrochar. *Energy and Fuels*, 34(11), 14147–14158. https://doi.org/10.1021/acs.energyfuels.0c01991

Zikri, A., Meigita, C., and Samosir, J. A. (2018). Characteristics of Biopellet from Variation of Raw Materials as Alternative Fuel, *Jurnal Kinetika*, 9(01), 26–32.

Zouari, M., Marrot, L., and DeVallance, D. B. (2024). Effect of demineralization and ball milling treatments on the properties of Arundo donax and olive stone-derived biochar. *International Journal of Environmental Science and Technology*, Springer Berlin Heidelberg, 21(1), 101–114. https://doi.org/ 10.1007/s13762-023-04968-9